Title

ATPase Copper Transporting Beta (ATP7B) Is a Novel Target for Improving the Therapeutic Efficacy of Docetaxel by Disulfiram/Copper in Human Prostate Cancer.

Journal

Molecular Cancer Therapeutics, 23(6)

ISSN

1535-7163

Authors

Song, Liankun

Nguyen, Vyvyan

Xie, Jun

et al.

Publication Date

2024-06-04

DOI

10.1158/1535-7163.mct-23-0876

Peer reviewed

Published in final edited form as:

Mol Cancer Ther. 2024 June 04; 23(6): 854–863. doi:10.1158/1535-7163.MCT-23-0876.

ATPase copper transporting beta (ATP7B) is a novel target for improving the therapeutic efficacy of docetaxel by disulfiram/copper in human prostate cancer

Liankun Song[1], **Vyvyan Nguyen**[1], **Jun Xie**[1], **Shang Jia**[2], **Christopher J. Chang**[2], **Edward Uchio**[1,3], **Xiaolin Zi**[1,3,4]

[1]Department of Urology, University of California, Irvine, Orange, CA 92868, USA

[2]Departments of Chemistry and Molecular and Cell Biology, University of California, Berkeley, Berkeley, CA 94720 USA

[3]Chao Family Comprehensive Cancer Center, University of California, Irvine, Orange, CA 92868, USA

[4]Veterans Affairs Long Beach Healthcare System, Long Beach, CA 90822, USA

Abstract

Docetaxel has been the standard first-line chemotherapy for lethal metastatic prostate cancer (mPCa) since 2004, but resistance to docetaxel treatment is common. The molecular mechanisms of docetaxel resistance remain largely unknown and could be amenable to interventions that mitigate resistance. We have recently discovered that several docetaxel-resistant mPCa cell lines exhibit lower uptake of cellular copper and uniquely express higher levels of a copper exporter protein ATP7B. Knock-down of ATP7B by silencing RNAs (siRNAs) sensitized docetaxel resistant-mPCa cells to the growth inhibitory and apoptotic effects of docetaxel. Importantly, deletions of ATP7B in human mPCa tissues predict significantly better survival of patients after their first chemotherapy than those with wild-type ATP7B ($P = 0.0006$). In addition, disulfiram (DSF), an FDA-approved drug for the treatment of alcohol dependence, in combination with copper, significantly enhanced the *in vivo* antitumor effects of docetaxel in a docetaxel-resistant xenograft tumor model. Our analyses also revealed that DSF and copper engaged with ATP7B to decrease protein levels of COMM domain-containing protein 1 (COMMD1), S-phase kinase-associated protein 2 (Skp2), and clusterin and markedly increase protein expression of cyclin-dependent kinase inhibitor 1 (p21/WAF1). Taken together, our results indicate a copper-dependent nutrient vulnerability through ATP7B exporter in docetaxel-resistant PCa for improving the therapeutic efficacy of docetaxel.

Keywords

Copper; Docetaxel Resistance; Disulfiram; ATP7B; Prostate Cancer

[*]**Address for correspondence:** Xiaolin Zi, Department of Urology, University of California, Irvine, 101 The City Drive South, Rt.81 Bldg.55 Rm.204, Orange, CA, 92868, USA. xzi@hs.uci.edu.

Conflict of Interest Disclosures: The authors declare no potential conflicts of interest.

Introduction

Taxanes (mainly docetaxel) are the first-line therapies prolonging the survival of metastatic prostate cancer (mPCa), which are often given to patients after the failure of androgen deprivation therapy (ADT) or second-generation anti-androgens [1, 2]. However, the benefits of docetaxel are often short-lived, and the disease continues to progress. After the development of resistance to Taxanes, there are very limited or no treatment options for metastatic castration-resistant PCa (mCRPC). Several mechanisms have been proposed for docetaxel resistance, including alterations of microtubules and androgen receptor (AR) signaling, activation of survival/anti-apoptotic pathways/apoptosis, enhanced antioxidant responses, reactivation of epithelial-to-mesenchymal transition and neuroendocrine differentiation, increasing cancer stemness and expression of Skp2 protein, and overexpression of membrane-bound drug efflux pumps, such as P-glycoprotein (P-gp/ABCB1), etc. [3–7]. Nevertheless, very limited progress has been made to improve the clinical efficacy of docetaxel in mPCa. Therefore, there is still an urgent need to identify new mechanisms of resistance to docetaxel for developing novel therapeutic combinations to improve its efficacy.

Along these lines, copper has emerged as an important metal nutrient in the initiation, progression, and treatment of cancer [8]. Copper is an essential trace element that is required for the proper functioning of various proteins including cytochrome-c oxidase, Mn21/Cu21 superoxide dismutase, and ceruloplasmin [9], with newer work pointing to a diverse array of transition metal signaling roles for this element [10, 11]. Indeed, this metal nutrient was found to be enriched (2 to 6-fold higher) in PCa cell lines and xenograft tumor models [12–15]. Because of the potential of copper achieving high accumulation in tumors, Positron emission tomography of $^{64}CuCl_2$ has been successfully used for detecting PCa recurrence in patients with low levels of prostate-specific antigen (PSA) [16]. Copper is a potent prooxidant and its excess causes the generation of cytotoxic reactive oxygen species (ROS) in cells [17].

Owing to its importance in cell proliferation and death pathways, copper homeostasis is tightly regulated. The uptake of copper into cells is mediated by the cell membrane protein copper transport protein 1 (CTR1) [18], whereas the secretion of intracellular copper is through copper-dependent ATPase transporters ATP7A and ATP7B. ATP7B consists of six metal-binding domains (MBDs), a nucleotide-binding domain (NBD), P-domain, A-domain, and a long c-terminal tail [19, 20]. ATP7B resides on the TransGolgi Network (TGN) through the stabilizing interaction between MBD and NBD [21, 22]. A loss of interaction between the MBD and the A-domain causes ATP7B to accumulate at the endoplasmic reticulum leading to intracellular copper accumulation [21, 22].

Disulfiram (DSF), an alcohol aversion drug, has been shown to be effective against different types of cancers in preclinical studies and the use of DSF was associated with reduced risk of cancer death in epidemiological studies [23–27]. DSF is metabolized into diethyldithiocarbamate and chelates with copper to form the diethyldithiocarbamate-copper complex (CuET) in vivo, which has been identified to be responsible for its anti-cancer effects [23]. DSF acts as a copper ionophore to increase copper bioavailability and has

displayed selective toxicity against PCa cells compared to normal prostate epithelial cells [24, 25].

In this study, we report that PCa cell lines with acquired resistance to docetaxel specifically expressed higher protein levels of ATP7B, which is accompanied by lower intracellular levels of copper. Knock-down of ATP7B by silencing RNAs re-sensitized docetaxel resistant-mPCa cells to the growth inhibitory and apoptotic effects of docetaxel. Interestingly, ATP7B deletion commonly occurs in human PCa tumor tissues and predicts better survival of PCa patients undergoing chemotherapies. In addition, we have shown that DSF/copper acts synergistically with docetaxel to inhibit the growth of PCa cells in both 2D and 3D cultures and xenograft models, as well as in a patient-derived PCa organoid culture. We also found that DSF engages with ATP7B, down-regulates its downstream events, such as copper metabolism MURR1 domain (COMMD1), α-clusterin, and S-phase kinase-associated protein 2 (Skp2), and up-regulates the expression of p21/WAF1. Taken together, this work establishes a copper-dependent nutrient vulnerability for augmenting cancer treatment, specifically targeting the copper-exporter protein ATP7B.

Materials and Methods

Cell lines and reagents:

DU145, 22Rv1, PC3, RWPE-1, C4–2B, MDA-PCa2B, PC3M-LN4, and LNCaP cell lines from American Type Culture Collection (ATCC, Manassas, VA) were maintained in RPMI-1640 media (Fisher Scientific) supplemented with 10% fetal bovine serum (FBS) and 1% penicillin-streptomycin. These cells were characterized and authenticated by ATCC. In addition, all cell lines were tested for known species of mycoplasma contamination using a kit from LONZA Inc. (Walkersville, MD) and used within 20 passages. The DU145-docetaxel resistant (DR), 22Rv1-DR, LNCaP-DR, and PC3-DR cell lines were gifts from Dr. Carlos Cordon-Cardo (Columbia University College of Physicians and Surgeons, Columbia University, New York). These docetaxel-resistant prostate cancer cell lines were established in the presence of escalating concentrations of docetaxel up to 250 nM until 6 to 9 months. Docetaxel with 99.42% purity was purchased from MedChemExpress LLC (Monmouth Junction, NJ). DSF and copper chloride ($CuCl_2$) were obtained from Sigma-Aldrich (St. Louis, MO). Copper Fluor-4 (CF4), a synthetic fluorophore for live-cell copper imaging, and Control Copper Fluor-4 S2 (Ctrl-CF4-S2) were synthesized by Dr. Shang Jia in the laboratory of Dr. Christopher J. Chang.

MTT assay.

Parental DU145 and DU145-DR were seeded at a density of 5,000 cells/well, and parental 22Rv1 and 22Rv1-DR cells at a density of 12,000 cells/well in 24 well plates. After 24 hours, DSF at indicated concentrations of 0, 20, 40, 80, 120, 160, 320, 500nM, and DSF plus 20μM $CuCl_2$ (DSF/copper) were applied to the cells. MTT (3-(4,5-dimethylthiazol-2-yl)-2,5-diphenyltetrazolium bromide) dissolved in PBS was added to each well for 2 hours after 72 hours of the treatments, and the absorbance was determined at 570 nm. Dose-response curves for cell viability were generated as a percentage of viability from vehicle control DMSO-treated cells. For the combined effect of docetaxel and DSF/copper,

DU145-DR and 22Rv1-DR cells were seeded in 48 well plates at the densities of 3000 and 5000 cells/well, respectively, and treated with docetaxel and DSF at indicated concentrations plus 20μM $CuCl_2$. Cell viabilities were measured by the MTT assay and evaluated in SynergyFinder Plus (www.synergyfinderplus.org). The combination effects were tested in models of HSA (highest single agent), BLISS (Bliss independence), LOEWE (Loewe additivity), and ZIP (zero interaction potency) for antagonist, additive, and synergistic effects as described in published paper [28].

Colony formation assay [29]:

Autoclaved 1.6% agarose solution was mixed with the same volume of 2X RPMI 1640 complete medium and used to create the base agarose layer in 6 well plates. DU145-DR and 22Rv1-DR were resuspended in 2X RPMI 1640 complete medium followed by mixing with 0.8% sterile agarose solution at the ratio of 1:1 to be plated on top of the base agarose layer. After gel solidification, RPMI 1640 complete medium containing 10 nM DSF and 20μM $CuCl_2$, 200nM docetaxel, or the combination of DSF/copper and docetaxel were added into each well and treated for 4–6 weeks. After the treatments, the cell colonies were fixed with methanol, stained with crystal violet, imaged, and counted. Percentages of colony formation relative to control treatment were calculated.

Fluorescence imaging of labile, cellular copper pools with selective copper-responsive dyes [30]:

The specific copper probes for imaging cellular copper were generated by Dr. Christopher J. Chang's lab at the University of California, Berkeley. Copper probe CF4 and control probe Ctrl-CF4-S2 were dissolved in methanol, aliquoted, and stored at −80°C. Parental DU145, DU145-DR, parental 22Rv1, and 22Rv1-DR cells were plated in 24 well plates. After 24 hours, the copper chloride was added for 2 hours in serum-free media before imaging. The cells were then washed to remove any excess copper in the media and then incubated with CF4 copper and Ctrl-CF4-S2 control probes at 0.5μM for 20 minutes. The photos were taken under a Keyence BZX 7000 fluorescence microscope with a 40X objective lens. CF4 has its largest fluorescence turn-on when excited at 536 nm. Ten fields of cells per well were used to obtain the average fluorescence intensity and the fluorescence intensities were analyzed by Image J software. Each treatment included three replicates per experiment and each experiment was performed 3–5 times to obtain biological replicates.

Western blotting analysis:

Cells were lysed in RIPA buffer with protease inhibitors and protein concentrations were determined by the Bio-Rad DC protein assay. An equal total amount of protein was loaded onto SDS-PAGE gels and then transferred onto PVDF membranes. After blocking with 5% non-fat milk, the membranes were probed with antibodies against ATP7B, ATP7A, COMMD1, α-clusterin, β-tubulin (Santa Cruz Biotechnology, Dallas, TX), Skp2 (Invitrogen, Grand Island, NY), PARP (Cell signaling technology, Danvers, MA), p21 and CTR1 (Abcam, Inc., Waltham, MA) overnight at 4°C. Membranes were washed and incubated with corresponding anti-mouse or anti-rabbit secondary antibodies for 2 hours at room temperature. The blots were visualized by an enhanced chemiluminescence detection system. β-tubulin was used as a loading control.

Knockdown of ATP7B and COMMD1 by siRNAs:

Human ATP7B, COMMD1, and control siRNAs were purchased from Qiagen. Cells were transfected with these siRNAs by lipofectamine 3000 (Thermo Fisher Scientific, Waltham, MA) in 48 well and 6 well plates. After 48 hours of transfection, the cells were treated with docetaxel at indicated concentrations for 24 or 72 hours. Protein expression and cell viability were evaluated by Western blotting analysis and MTT assay, respectively.

PCa Patient-derived organoid (PDO):

Human PCa tissues were obtained from prostatectomy specimens under the University of California, Irvine Institutional Review Board protocol #2000–1296 and with patients' written consent. The studies were conducted according to the Declaration of Helsinki Principles and Good Clinical Practice by the International Conference on Harmonization guidelines. The tissues were cut into small pieces with a scalpel and digested in 5 mg/ml collagenase II with 10μM Y-27632 in a 15 ml tube for 2 hours at 37°C with shaking. After washing with adDMEM/F12+/+/+ (containing penicillin/streptomycin, 10mM Hepes and GlutaMAX) and centrifugation, the pellets were further digested in TrypLE with 10μM Y-27632 for approximately 15 minutes at 37°C, pipetting up and down every 5mins, afterward, performing wash and centrifugation again, the digested cells were counted, resuspended in cold Matrigel and plated 20μl/well into 48 well plates or 10μl/well into 96 well plates. Putting the plates upside down in the 37°C incubator for 15 min to allow the Matrigel to solidify. 300μl or 100μl of pre-warmed human prostate culture medium plus 10μM Y-27632 was added into each well. The medium was refreshed every 3 days and TrypLE was used for passaging. All the cultural procedures and conditions followed the published protocol [31]. Organoids derived from human Pca tissues were passed into 96 well plates, and whole-well z-stack images were acquired at day 0 using Keyence fluorescence microscopy before treatments. Organoids in the same area as day 0 were imaged at indicated time points after treatments. Medium with DMSO control or drugs was refreshed every 3 days. The sizes of organoids were analyzed by Image J software to assess the morphological effects of the treatments.

In vivo xenograft tumorigenesis assay [32].

22Rv1-DR cells were resuspended in PBS and mixed with Matrigel (Corning, NY, USA) at the ratio of 1: 1, and then injected subcutaneously into the right flank of male NOD/SCID mice (Charles River Laboratories, Wilmington, MA, USA), respectively. Mice at a mean weight of 25 g were randomly assigned into four treatment groups when tumors reached around 200 mm^3, including vehicle control, 10 mg/kilogram (Kg) docetaxel weekly by intraperitoneal injection (IP), 1 mg/kg/day $CuCl_2$ by IP injection plus 100mg/kg/day DSF via gavage and the combination of both. The body weights and tumor volumes were measured every 3 days. Mice were euthanized before the humane endpoint was reached by CO_2 asphyxiation and cervical dislocation, and tumor tissues were collected and weighed. Institutional guidelines and the IACUC-approved protocol by the University of California, Irvine (protocol #2007–2740) were followed for animal care and treatments. A sample size of 5 mice in each group allows 80% power to detect a 30% difference in tumor weight.

Immunohistochemistry (IHC) and Immunofluorescence (IF) Staining Assays [32]:

Tumor tissues are fixed in 10% formalin, paraffin-embedded, and sectioned at 5-μm thickness. Sections were deparaffinized, hydrated, and incubated in a steamer for 20 minutes in a sodium citrate buffer for antigen retrieval. Then, they were quenched with 3% hydrogen peroxide for 10 minutes followed by washing thrice using PBS and incubated with 3% normal goat serum blocking for 1 hour. After that, the slides were incubated with primary antibodies, including anti-Ki67 (1:100), anti-ATP7B (1:150), and anti-AR (1:100) overnight at 4°C. After rinsing with 0.1% tween 20-PBS three times and incubating with horseradish peroxidase (HRP)-labeled secondary antibody, sections were visualized with 3, 3-diaminobenzidine using the Cell and Tissue Staining kit (R&D Systems, Minneapolis, MN) and cover-slipped. Images were taken under Keyence BZX710 microscope. The number of positive-stained cells per field under the ×40 objective lens was counted and averaged from 25 fields of five tumors in each group in a blind way. Error bars were standard deviations.

Statistical analysis [32]:

Experiments were repeated independently more than three times, and mean values from each group were analyzed for significant differences, data were presented as means ± standard deviation or standard errors. Two-tailed student's t-test or one-way ANOVA (Analysis of Variance) was performed for statistical analysis, P value <0.05 was considered significant.

Data Availability Statement:

The data generated in this study are available within the article and its supplementary data files.

Results

ATP7B deep deletion predicts better survival of mPCa patient after their first chemotherapy and its over-expression is associated with PCa cells acquiring resistance to docetaxel.

From the publicly available metastatic prostate adenocarcinoma datasets, including "MCTP, Nature 2012", "SU2C/PCF Dream Team, PNAS 2019", and "The Metastatic Prostate Cancer Project, Provisional, June 2021", 21.31% (13 out of 61), 9.91% (44/444) and 6.1% (5/82) cases, respectively, exhibit ATP7B deep deletion (*i.e.,* homozygous deletion) (Figure 1A) [33]. Primary PCa samples from datasets of "the TCGA, Firehose Legacy", "Fred Hutchinson CRC, Nat Med 2016", "SMMU, Eur Urol 2017", and "MSK, Cancer Cell 2010" show 16.03% (80/499), 10.4% (16/154), 6.2% (4/65), and 4.2% (9/213) cases, respectively, with ATP7B deep deletion (Figure 1A) [https://www.cbioportal.org/results/cancerTypesSummary?cancer_study_list=prad_mich%2Cprad_su2c_2019%2Cprad_tcga&Z_SCORE_THRESHOLD=2.0&RPPA_SCORE_THRESHOLD=2.0&profileFilter=mutations%2Cstructural_variants%2Ccna%2Cgistic&case_set_id=all&gene_list=ATP7B&geneset_list=%20&tab_index=tab_visualize&Action=Submit.]. Cumulative survival analysis of mPCa patients after their first chemotherapy in the dataset of "SU2C/PCF Dream Team, PNAS 2019" revealed that the median survival time of mPCa patients with ATP7B deletion was significantly longer

than mPCa patients carrying wild-type ATP7B (120 vs. 38 months) (P=0.0006). These results suggest that ATP7B deletion is relatively common in PCa tumors and may be an important and clinically significant target for overcoming resistance to chemotherapies in PCa.

We therefore have examined the expression of ATP7B and other copper regulators in paired parental and docetaxel-resistant PCa cell lines. Figure 1C shows that docetaxel-resistant mPCa cell lines DU145-DR, 22Rv1-DR, LNCaP-DR, and PC3-DR all exhibited markedly higher protein levels of ATP7B compared to their parent cell lines. There are no marked differences in protein levels of CTR1 among these cell lines, but the protein levels of ATP7A are lower in LNCaP-DR and PC3-DR cells compared to parental LNCaP and PC3 cells. ATP7B expression in parental C4–2B and MDA-PCa2B (a cell derived from African American prostate cancer) cells was not detected while strong protein expression of ATP7B is shown in RWPE-1 (an immortalized prostate epithelial cell line) and PC3M-LN4 cells (Supplementary Figure 1). In Figure 1D, suppression of ATP7B expression by siRNAs resulted in enhanced sensitivity of docetaxel-resistant DU145-DR cells to the growth inhibitory effects of docetaxel by more than 20-fold (IC_{50s} for siRNA control *vs.* ATP7B siRNAs are 567.7 ± 23. 2 nM *vs.* 25. 4 ± 7.7 nM, $P < 0.001$). The IC_{50s} of docetaxel for the growth of parental DU145 cells with siRNA control or ATP7B siRNA transfection are 4.69 ± 0.08 nM *vs.* 1.67 ± 0.07 nM (Supplementary Figure 2). DU145- DR cells are about 121-fold less sensitive to the growth inhibitory effects of docetaxel compared to parental DU145 cells (Supplementary Figure 2). Western blotting analysis of PARP cleavage (a hallmark of apoptosis) further revealed that suppression of ATP7B by siRNAs led to enhanced PARP cleavage by docetaxel (Figure 1E). These findings indicate that ATP7B overexpression is a key factor in docetaxel-resistant PCa cells and knock-down of ATP7B by siRNAs re-sensitizes the resistant PCa cells to the growth inhibitory and apoptotic effect of docetaxel.

Acquired docetaxel resistance in PCa cells is associated with reduced copper uptake; ATP7B siRNAs, DSF, and docetaxel treatments increase the cellular uptake of copper.

We next used a novel, copper-selective fluorescent probe (Copper Fluor-4, CF4) to examine intracellular pool levels of labile copper and determine whether labile copper levels are related to resistance or responses to the docetaxel treatment in PCa cell lines. Interestingly, the data in Figures 2A and B show that both DU145-DR and 22Rv1-DR cells accumulate markedly less (about 2 to 4-fold) copper compared to parent DU145 and 22Rv1 cells (Ps < 0.001) and that DU145-DR has a significantly lower basal level of labile copper than parental DU145 cells ($P < 0.001$).

Given that ATP7B protein levels are uniquely increased in docetaxel-resistant PCa cell lines and that the copper efflux transporter ATP7B pumps copper out of the cell to maintain cellular homeostasis requirements, Figure 2C confirms that suppression of ATP7B levels by siRNA in docetaxel-resistant DU145-DR cells results in a significant increase in intracellular copper levels by 1.3 to 2.1-fold (Ps< 0.05), compared to control siRNA transfection.

DSF can act as a copper ionophore to facilitate the transport of copper specifically into tumor tissues and to increase the levels of intracellular copper [33]. Therefore, we also

examined the effects of DSF, docetaxel, and their combination on the intracellular levels of labile copper in PCa cell lines. Figure 2D shows that DSF and the combination of DSF and docetaxel both elevated the levels of intracellular copper by 3.4 and 33.5-fold, respectively, compared to vehicle control treatment (Ps < 0.01).

Docetaxel-resistant PCa cell lines are more sensitive to the growth inhibitory effects of DSF and DSF/copper; DSF/copper acts synergistically with docetaxel to inhibit PCa cell growth.

Given that docetaxel-resistant PCa cell lines have reduced intracellular copper levels and that DSF is a copper ionophore, we proceeded to evaluate the effect of DSF and DSF/$CuCl_2$ on the growth of DU145-DR and 22Rv1-DR cells and their parental cell lines. Figures 3A and 3B show that docetaxel-resistant mPCa DU145-DR and 22Rv1-DR cells are more sensitive to the growth inhibitory effects of both DSF alone and DSF/$CuCl_2$ compared to their parent cells. The IC_{50s} of the DSF/$CuCl_2$ combination are 11.45 ± 1.2 nM and 90.93 ± 5.4 nM for DU145-DR and 22Rv1-DR cells compared to 69.0 ± 5.3 nM and 117.00 ± 5.4 nM for parental DU145 and 22Rv1 cells, respectively (Ps < 0.05). The addition of Cu salt enhanced the growth inhibitory effects of DSF in all tested cell lines (Figures 3A and 3B and supplementary table 1). These results suggest the high potency and selectivity of DSF/$CuCl_2$ combination to inhibit the growth of docetaxel-resistant mPCa cells.

We next evaluated the combined effect of DSF/$CuCl_2$ and docetaxel on cell growth. The combination treatments induced greater cytotoxicity than the sum of DSF/$CuCl_2$ and docetaxel was given alone at their suboptimal concentrations and resulted in the average highest single agent (HAS) synergy scores of 11.24 and 36.56 for DU145-DR and 22Rv1-DR cells, respectively (Figures. 3C and D, Ps < 0.0001), indicating strong synergistic effects.

DSF/copper acts synergistically with docetaxel to inhibit the growth of 3 dimensional (3D) cultures of docetaxel-resistant cell lines and PCa PDOs.

When anchorage-independent 22Rv1-DR and DU145-DR cell growth was assayed in soft agar, docetaxel alone at a concentration of 200 nM for 6 weeks did not inhibit colony formation, 10 nM DSF/20 μM $CuCl_2$ reduced colony formation by 41 to 45%, and the combination reduced colony formation by more than 90% (Figures 4 A and B), which was statistically significantly greater (P<0.0001) than growth inhibition with either docetaxel alone or DSF/$CuCl_2$.

We have also developed PCa patient-derived organoid (PDOs) cultures from fresh prostatectomy specimens of an African-American patient diagnosed with PCa. The purity and Gleason grade of the PCa tissue were examined by a board-certified pathologist (B.W.), who confirmed the specimen with Gleason grade 4+3. We then used pure PCa tissues to develop PDO cultures and tested the growth-inhibitory effects of docetaxel, DSF/$CuCl_2$, and their combination. H&E staining reveals similar histology between the patient's tumor and the PDO (Supplementary Figure 3). The PDOs also express higher levels of ATP7B and androgen receptor proteins (Supplementary Figure 3). The average size of the PDOs grew by 72% under vehicle control (DMSO) treatment for 4 days, while the mean size of

the PDO remained unchanged under docetaxel treatment and decreased by approximately 24% after DSF/$CuCl_2$ treatment for 5 days (Figures 4C and D). The combination treatment reduced the mean size of the PDO by more than 55%, which is more effective than docetaxel or DSF/$CuCl_2$ treatment alone (Figures 4C and D) (Ps < 0.05). These results suggest that DSF/$CuCl_2$ can re-sensitize or enhance docetaxel's effects against the growth of PCa PDOs with high expression of ATP7B.

IHC staining further shows that DSF/$CuCl_2$ and docetaxel combination-treated PDOs exhibit fewer Ki67-positive cells and more cleaved-caspase 3-positive cells (Figure 4E), suggesting the antiproliferative and apoptotic effects of the combination.

DSF/copper engages with ATP7B and disrupts its non-canonical downstream events.

We next evaluate drug target interactions of DSF or copper with ATP7B using a cellular thermal shift assay [34, 35]. Figure 5A shows that both DSF and $CuCl_2$ treatments significantly shielded ATP7B from degradation at 62°C at the optimal peak concentrations of 200 nM and 20 μM, respectively. ATP7B protein levels were elevated in a concentration-dependent manner after heating at an optimal temperature of 62°C (Fig. 5B). These results strongly suggest that both DSF and copper directly bind to ATP7B in DU145-DR cells.

In addition to exporting copper, emerging evidence indicates that ATP7B can regulate proteostatic functions and apoptosis by interacting with COMMD1 and clusterin [20–22]. COMMD1 promotes cullin-based ubiquitination and regulates the Skp2 E3 ligase complex [36]. Clusterin is associated with the clearance of cellular debris and apoptosis [37]. Figure 5C demonstrates that COMMD1, clusterin, and Skp2 protein were markedly down-regulated, whereas p21/WAF1 was dose-dependently increased by DSF/ $CuCl_2$ treatments. The downregulation of Skp2 protein expression by DSF/ $CuCl_2$ was partly attenuated by the knockdown of COMMD1 expression using specific siRNAs (Supplementary Figure 4), suggesting that Skp2 may be a down-stream event of ATP7B/COMMD1. Taken together, these results indicate that the DSF/copper interacts with ATP7B leading to disruption of the downstream events of ATP7B.

These results support a model shown in Figure 5D, wherein docetaxel-resistant PCa cells exhibit elevated protein levels of ATP7B, which leads to reduced intracellular copper levels and activation of ATPase-independent function of ATP7B through clusterin, COMMD1, and Skp2, and then collectively result in cell survival and resistance to apoptosis. DSF or copper binds to ATP7B not only increasing intracellular copper levels but also decreasing the expression of clusterin, COMMD1, and Skp2 and upregulation of p21/WAF1, which induces apoptosis and cell growth inhibition.

DSF/copper effectively inhibits tumor growth and re-sensitizes the anti-tumor effect of docetaxel in a docetaxel-resistant mPCa xenograft model.

Figure. 6A. shows that docetaxel plus DSF/ $CuCl_2$ treatments result in a highly significant decrease in the growth rate of 22Rv1-DR tumors compared with vehicle control, DSF/ $CuCl_2$, or docetaxel alone (ANOVA, Ps < 0.001). The combination resulted in more than 65% inhibition of tumor growth (Figure 6A). The tumor weights of 22Rv1-DR xenografts in control, docetaxel, DSF/$CuCl_2$, and docetaxel plus DSF/$CuCl_2$ groups recorded at the

end of the treatment were 1.77 ± 0.18, 1.29 ± 0.42, 1.23 ± 0.46, and 0.56 ± 0.35 g (mean tumor weight ± SD), respectively. DSF/$CuCl_2$ significantly enhanced the antitumor efficacy of docetaxel by approximately 40%. (Student's t-test, $P < 0.001$; Figures. 6B and C).

To examine whether these treatments affected ATP7B expression and cell proliferation and apoptosis *in vivo* situations, tumor xenograft tissue sections were analyzed by IHC for ATP7B, Ki67, a marker for cell proliferation, and cleaved Caspase-3, a marker for apoptotic cells (Figure 6D). IHC staining for ATP7B revealed focal, membranous, and cytoplasmic staining. There is no statistical significance in the expression of ATP7B protein in tumor tissues from different treatment groups (Ps > 0.05). The quantification of Ki67- and cleaved Caspase-3 positive cells in tumor sections showed a decrease in cell proliferation and an increase in apoptotic cells in the docetaxel, DSF/$CuCl_2$, and the combination treatment groups compared to control (Figure 6E, Ps < 0.01). In addition, the combination treatment is more effective than docetaxel alone or DSF/ $CuCl_2$ in reducing cell proliferation and in induction of apoptosis (Figure 6E, Ps < 0.01). H&E staining shows different cell morphologies in tumor tissues among different treatment groups (Supplementary Figure 5), suggesting potential mechanistic differences among these treatments. In addition, DSF/ $CuCl_2$ treatment reduced the protein expression of COMMED1, Skp2, and α-Clusterin and increased the expression of p21/WAF1 (Supplementary Figure 6). This result is consistent with our in vitro findings as shown in Figure 4C.

Discussion

The *ATP7B* gene that encodes a copper-transporting P-type ATPase containing 1465 amino acids is located on chromosome 13q14.3. Several well-known tumor suppressor genes in PCa, including *BRCA2*, *RB1,* and *FOXO1A*, are also located on the q14 band of chromosome 13 (13q14) [38]. Allelic loss at 13q14 was found in about one-third of prostate tumors, which is one of the most frequent deletions in PCa [38]. Therefore, not surprisingly, *ATP7B* deep deletion exists in about 4% to 21% of prostate tumors in different patient populations and appears to be more frequently found in prostate tumors compared to other cancers. Genetic disorders of the *ATP7B* gene damage the copper excretion pathway, which results in irregular copper accumulation in the liver, cornea, joints, kidney, and heart muscle, contributing to Wilson's disease's clinical features [39]. However, the potential functional roles of ATP7B in prostate tumors remain largely unknown. In this study, we analyzed the data from the publicly available dataset of "SU2C/PCF Dream Team, PNAS 2019" and the result indicates that *ATP7B* deletion predicts better survival of PCa patients after their first chemotherapy (mainly docetaxel treatment). In addition, all examined docetaxel-resistant PCa cell lines that were developed by exposure to docetaxel treatment for a long period express much higher levels of ATP7B protein accompanied by reduced intracellular copper levels compared to their parent cell lines. Suppression of ATP7B expression by siRNAs increases intracellular copper levels and re-sensitizes docetaxel resistant-PCa cells to the growth inhibitory and apoptotic effects of docetaxel both *in vitro* and *in vivo*. Multiple mechanisms have been reported to contribute to the docetaxel resistance in PCa, including alterations in microtubule-protein interactions, over-expression, and higher activity of multidrug efflux transporters of the ABC superfamily including P-glycoprotein (P-gp/ABCB1), activation of AR signaling and expression of AR V7, overexpression of

TMPRSS2-ERG fusion protein, enrichment of cancer stem cells, etc [3–7]. In this study, our results have indicated up-regulation of ATP7B protein leading to reduced intracellular copper levels as a new mechanism of developing docetaxel resistance. Therefore, targeting ATP7B could be a new strategy for overcoming docetaxel resistance in human PCa.

DSF is a Federal Drug Administration (FDA) approved, well-tolerated, and inexpensive drug to treat alcohol dependence since 1951 through blocking acetaldehyde dehydrogenase that converts acetaldehyde to a harmless acetic acid [23–26]. Recently, there has been an increasing interest in repurposing DSF as a cost-effective anticancer drug as it has demonstrated anti-tumor activities in a wide variety of cancers [23–26]. DSF also acts as a copper ionophore to raise its intracellular levels. The cytotoxic effects of DSF are dependent on intracellular copper levels and its anti-tumor activity can be enhanced by dietary supplementation of copper. Given tumor cells often contain higher levels of cellular copper than normal cells, DSF can selectively inhibit the growth of cancer cells but not normal healthy cells [33]. DSF reacts with copper to form a potent anti-cancer component bis-diethyladithio-carbamate (DDC_2) copper complex [Cu $(DDC)_2$ also named as CuET], which targets the nuclear protein localization protein 4 (NPL4) component of the p97 segregase leading to accumulation of polyubiquitylated (polyUb) proteins, and inhibits the NF-κB pathway, as well as induces cytotoxic ROS [23]. In this study, we found that DSF engagement with ATP7B complex not only led to increased cellular uptake of copper but also down-regulation of several ATPase independent down-stream components of ATP7B, including α-clusterin and COMMD1/Skp2 in docetaxel resistant PCa cells. Our findings have provided new mechanisms by which DSF/copper overcome the resistance of PCa cells to docetaxel and enhance the anti-tumor efficacy of docetaxel in PCa. Currently, it is still unknown how docetaxel treatment results in an increased expression of ATP7B in PCa cells. Recently, Petruzzelli et al [40] have reported that transcription factor EB (TEFB) is a key transcriptional factor for controlling *ATP7B* gene expression. In addition, Zhang et al [41] have shown that docetaxel regulates TFEB nuclear translocation and its transcriptional activity. Therefore, we are testing the hypothesis that docetaxel increases TFEB nuclear localization and its transcription activity leading to upregulation of ATP7B and drug resistance in prostate cancer. Further studies are in progress to investigate a potential link between docetaxel treatment and ATP7B expression or copper transportation.

DSF and DSF/copper as a single modality in several phase I or II trials have been judged unsuccessful [42]. In addition, large research efforts, including clinical trials, have been performed to identify additional agents to combine with docetaxel to improve clinical outcomes [43–46]. Although any agent that could further enhance the response rate to docetaxel would be a significant improvement in patient outcomes, very little progress has been made during the past 18 years [43–46]. Instead of using the single modality, our results have demonstrated that DSF/copper acts synergistically with docetaxel to potently inhibit the growth of docetaxel-resistant PCa cell lines and significantly enhance the in vivo anti-tumor efficacy of docetaxel in 3D cultures of PCa patient-derived organoids and docetaxel resistant xenograft models. Since there are currently no effective treatment modalities after the development of docetaxel resistance, the combination of DSF/copper and docetaxel deserves further clinical investigation.

In summary, we have identified that ATP7B is a potential determining factor for docetaxel resistance or responses through regulation of intracellular copper levels and its downstream events, including α-clusterin and COMMD1/Skp2 leading to cell survival and proliferation. DSF/dietary copper overcomes docetaxel resistance and acts synergistically with docetaxel to enhance its anti-tumor effects. DSF/copper has the potential to be repurposed to enhance docetaxel-based therapy for the treatment of advanced PCa even after patients fail chemotherapy.

Supplementary Material

Refer to Web version on PubMed Central for supplementary material.

Acknowledgment:

This work was supported in part by NIH 1R01 CA260351–02 and VA merit award I01BX005105 (to X. Zi.) and NIH R01 GM79465–18 (to C.J.C.). C.J.C. is a CIFAR Fellow. In addition, the authors acknowledge support from the Chao Family Comprehensive Cancer Center (NCI award P30CA62203) and its shared resources.

References:

1. Kyriakopoulos CE, Chen YH, Carducci MA, Liu G, Jarrard DF, Hahn NM, et al. Chemohormonal Therapy in Metastatic Hormone-Sensitive Prostate Cancer: Long-Term Survival Analysis of the Randomized Phase III E3805 CHAARTED Trial. J Clin Oncol. 2018; 36: 1080–1087. [PubMed: 29384722]
2. Kinsey EN, Zhang T, Armstrong AJ. Metastatic Hormone-Sensitive Prostate Cancer: A Review of the Current Treatment Landscape. Cancer J. 2020; 26:64–75. [PubMed: 31977388]
3. Gjyrezi A, Xie F, Voznesensky O, Khanna P, Calagua C, Bai Y, et al. Taxane resistance in prostate cancer is mediated by decreased drug-target engagement. J Clin Invest. 2020; 130:3287–3298. [PubMed: 32478682]
4. Mout L, Moll JM, Chen M, de Morrée ES, de Ridder CMA, Gibson A, et al. Androgen receptor signalling impairs docetaxel efficacy in castration-resistant prostate cancer. Br J Cancer. 2020;123:1715–1719. [PubMed: 32989230]
5. Martin SK, Kyprianou N. Exploitation of the Androgen Receptor to Overcome Taxane Resistance in Advanced Prostate Cancer. Adv Cancer Res. 2015; 127:123–58. [PubMed: 26093899]
6. Marín-Aguilera M, Codony-Servat J, Reig Ò, Lozano JJ, Fernández PL, Pereira MV, et al. Epithelial-to-mesenchymal transition mediates docetaxel resistance and high risk of relapse in prostate cancer. Mol Cancer Ther. 2014;13:1270–84. [PubMed: 24659820]
7. Lombard AP, Liu C, Armstrong CM, Cucchiara V, Gu X, Lou W, et al. ABCB1 Mediates Cabazitaxel-Docetaxel Cross-Resistance in Advanced Prostate Cancer. Mol Cancer Ther. 2017; 16:2257–2266. [PubMed: 28698198]
8. Ge EJ, Bush AI, Casini A, Cobine PA, Cross JR DeNicola GM, et al. Connecting copper and cancer: from transition metal signaling to metalloplasia, Nature Rev Cancer 2022; 22: 102–113. [PubMed: 34764459]
9. Milne DB. Copper intake and assessment of copper status. Am J Clin Nutr. 1998; 67 (5 Suppl):1041S–1045S. [PubMed: 9587149]
10. Chang CJ “Searching for Harmony in Transition-Metal Signaling”, Nature Chem. Biol. 2015, 111, 744–747.
11. Pham VN; Chang CJ “Metalloallostery and Transition Metal Signalling: Bioinorganic Copper Chemistry Beyond Active Sites”, Angew. Chem. Int. Ed. 2023, 62, e202213644.
12. Denoyer D, Pearson HB, Clatworthy SA, Smith ZM, Francis PS, Llanos RM, et al. Copper as a target for prostate cancer therapeutics: copper-ionophore pharmacology and altering systemic copper distribution. Oncotarget. 2016;7:37064–37080. [PubMed: 27175597]

13. Chen D, Cui QC, Yang H, Barrea RA, Sarkar FH, Sheng S, et al. Clioquinol, a therapeutic agent for Alzheimer's disease, has proteasome-inhibitory, androgen receptor-suppressing, apoptosis-inducing, and antitumor activities in human prostate cancer cells and xenografts. Cancer Research. 2007;67:1636–1644. [PubMed: 17308104]

14. Safi R, Nelson ER, Chitneni SK, Franz KJ, George DJ, Zalutsky MR, et al. Copper signaling axis as a target for prostate cancer therapeutics. Cancer Research. 2014;74:5819–5831. [PubMed: 25320179]

15. Cai H, Wu JS, Muzik O, Hsieh JT, Lee RJ, Peng F. Reduced ^{64}Cu uptake and tumor growth inhibition by knockdown of human copper transporter 1 in xenograft mouse model of prostate cancer. Journal of Nuclear Medicine. 2014; 55:622–628. [PubMed: 24639459]

16. Singh A, Kulkarni HR, Baum RP. Imaging of Prostate Cancer Using 64Cu-Labeled Prostate-Specific Membrane Antigen Ligand. PET Clin. 2017; 12: 193–203. [PubMed: 28267453]

17. Zubair H, Khan HY, Sohail A, Azim S, Ullah MF, Ahmad A, et al. Redox cycling of endogenous copper by thymoquinone leads to ROS-mediated DNA breakage and consequent cell death: putative anticancer mechanism of antioxidants. Cell Death Dis. 2013; 4: e660. [PubMed: 23744360]

18. Puig S, Lee J, Lau M, Thiele DJ. Biochemical and genetic analyses of yeast and human high affinity copper transporters suggest a conserved mechanism for copper uptakeJ Biol Chem. 2002 Jul 19;277(29):26021–3019. [PubMed: 11983704]

19. Das S, Mohammed A, Mandal T, Maji S, Verma J, Ruturaj, et al. Polarized trafficking and copper transport activity of ATP7B: A mutational approach to establish genotype-phenotype correlation in Wilson disease. Hum Mutat. 2022; 43:1408–1429. [PubMed: 35762218]

20. Bitter RM, Oh S, Deng Z, Rahman S, Hite RK, Yuan P. Structure of the Wilson disease copper transporter ATP7B. Sci Adv. 2022; 8: eabl5508. [PubMed: 35245129]

21. Hasan NM, Gupta A, Polishchuk E, Yu CH, Polishchuk R, Dmitriev OY, et al. Molecular events initiating exit of a copper-transporting ATPase ATP7B from the trans-Golgi network. J Biol Chem. 2012; 287:36041–50.22. [PubMed: 22898812]

22. Stewart DJ, Short KK, Maniaci BN, Burkhead JL. COMMD1 and PtdIns(4,5)P2 interaction maintain ATP7B copper transporter trafficking fidelity in HepG2 cells. J Cell Sci. 2019;132: jcs231753.23. [PubMed: 31515276]

23. Skrott Z, Mistrik M, Andersen KK, Friis S, Majera D, Gursky J, et al. Alcohol-abuse drug disulfiram targets cancer via p97 segregase adaptor NPL4. Nature. 2017; 552:194–199. [PubMed: 29211715]

24. Hu JJ, Liu X, Xia S, Zhang Z, Zhang Y, Zhao J, et al. FDA-approved disulfiram inhibits pyroptosis by blocking gasdermin D pore formation. Nat Immunol. 2020; 21:736–745.25. [PubMed: 32367036]

25. Askgaard G, Friis S, Hallas J, Thygesen LC, Pottegård A. Use of disulfiram and risk of cancer: a population-based case-control study. Eur J Cancer Prev. 2014; 23:225–32 [PubMed: 23863824]

26. Sharma V, Verma V, Lal N, Yadav SK, Sarkar S, Mandalapu D, et al. Disulfiram and its novel derivative sensitize prostate cancer cells to the growth regulatory mechanisms of the cell by re-expressing the epigenetically repressed tumor suppressor-estrogen receptor β. Mol Carcinog. 2016; 55: 1843–1857. [PubMed: 26599461]

27. Cater MA, Haupt Y. Clioquinol induces cytoplasmic clearance of the X-linked inhibitor of apoptosis protein (XIAP): therapeutic indication for prostate cancer. Biochem J. 2011; 436: 481–91. 28. [PubMed: 21426304]

28. Ianevski A, Giri AK, Aittokallio T. SynergyFinder 3.0: an interactive analysis and consensus interpretation of multi-drug synergies across multiple samples. Nucleic Acids Res. 2022; 50: W739–W743. [PubMed: 35580060]

29. Zi X, Guo Y, Simoneau AR, Hope C, Xie J, Holcombe RF, et al. Expression of Frzb/secreted Frizzled-related protein 3, a secreted Wnt antagonist, in human androgen-independent prostate cancer PC-3 cells suppresses tumor growth and cellular invasiveness. Cancer Res. 2005; 65: 9762–70.30. [PubMed: 16266997]

30. Pezacki AT, Matier CD, Gu X, Kummelstedt E, Bond SE, Torrente L, et al. Oxidation state-specific fluorescent copper sensors reveal oncogene-driven redox changes that regulate labile copper(II) pools. Proc Natl Acad Sci U S A. 2022; 119: e2202736119. [PubMed: 36252013]

31. Drost J, Karthaus WR, Gao D, Driehuis E, Sawyers CL, Chen Y, et al. Organoid culture systems for prostate epithelial and cancer tissue. Nat Protoc. 2016;11:347–58. [PubMed: 26797458]

32. Song L, Mino M, Yamak J, Nguyen V, Lopez D, Pham V, et al. Flavokawain A Reduces Tumor-Initiating Properties and Stemness of Prostate Cancer. Front Oncol. 2022; 12:943846. [PubMed: 35912174]

33. Ekinci E, Rohondia S, Khan R, Dou QP. Repurposing Disulfiram as An Anti-Cancer Agent: Updated Review on Literature and Patents. Recent Pat Anticancer Drug Discov. 2019;14: 113–132. [PubMed: 31084595]

34. Li X, Pham V, Tippin M, Fu D, Rendon R, Song L, et al. Flavokawain B targets protein neddylation for enhancing the anti-prostate cancer effect of Bortezomib via Skp2 degradation. Cell Commun Signal. 2019; 17:25. [PubMed: 30885218]

35. Martinez Molina D, Jafari R, Ignatushchenko M, Seki T, Larsson EA, Dan C, et al. Monitoring drug target engagement in cells and tissues using the cellular thermal shift assay. Science. 2013; 341:84–7. [PubMed: 23828940]

36. Malek E, Abdel-Malek MA, Jagannathan S, Vad N, Karns R, Jegga AG, et al. Pharmacogenomics and chemical library screens reveal a novel SCFSKP2 inhibitor that overcomes Bortezomib resistance in multiple myeloma. Leukemia. 2017; 31:645–653. [PubMed: 27677741]

37. Muhammad LA, Saad F. The role of clusterin in prostate cancer: treatment resistance and potential as a therapeutic target. Expert Rev Anticancer Ther. 2015; 15:1049–61. [PubMed: 26313417]

38. Cooney KA, Wetzel JC, Merajver SD, Macoska JA, Singleton TP, Wojno KJ. Distinct regions of allelic loss on 13q in prostate cancer. Cancer Res. 1996; 56: 1142–5. [PubMed: 8640774]

39. Członkowska A, Litwin T, Dusek P, Ferenci P, Lutsenko S, Medici V, et al. Wilson disease. Nat Rev Dis Primers. 2018; 4: 21. [PubMed: 30190489]

40. Petruzzelli R, Mariniello M, De Cegli R, Catalano F, Guida F, Di Schiavi E, et al. TFEB Regulates ATP7B Expression to Promote Platinum Chemoresistance in Human Ovarian Cancer Cells. Cells. 2022; 11:219. [PubMed: 35053335]

41. Zhang J, Wang J, Wong YK, Sun X, Chen Y, Wang L, et al. Docetaxel enhances lysosomal function through TFEB activation. Cell Death Dis. 2018; 9:614. [PubMed: 29795139]

42. Zhang T, Kephart J, Bronson E, Anand M, Daly C, Spasojevic I, et al. Prospective clinical trial of disulfiram plus copper in men with metastatic castration-resistant prostate cancer. Prostate. 2022; 82: 858–866. [PubMed: 35286730]

43. Beer TM, Hotte SJ, Saad F, Alekseev B, Matveev V, Fléchon A, et al. Custirsen (OGX-011) combined with cabazitaxel and prednisone versus cabazitaxel and prednisone alone in patients with metastatic castration-resistant prostate cancer previously treated with docetaxel (AFFINITY): a randomised, open-label, international, phase 3 trial. Lancet Oncol. 2017; 18:1532–1542. [PubMed: 29033099]

44. Vogelzang NJ, Beer TM, Gerritsen W, Oudard S, Wiechno P, Kukielka-Budny B, et al. VIABLE Investigators. Efficacy and Safety of Autologous Dendritic Cell-Based Immunotherapy, Docetaxel, and Prednisone vs Placebo in Patients With Metastatic Castration-Resistant Prostate Cancer: The VIABLE Phase 3 Randomized Clinical Trial. JAMA Oncol. 2022; 8:546–552. [PubMed: 35142815]

45. Tannock IF, Fizazi K, Ivanov S, Karlsson CT, Fléchon A, Skoneczna I, et al. ; VENICE investigators. Aflibercept versus placebo in combination with docetaxel and prednisone for treatment of men with metastatic castration-resistant prostate cancer (VENICE): a phase 3, double-blind randomised trial. Lancet Oncol. 2013; 14:760–8. [PubMed: 23742877]

46. Zhuang E, Uchio E, Lilly M, Zi X, Fruehauf JP. A phase II study of docetaxel plus lycopene in metastatic castrate-resistant prostate cancer. Biomed Pharmacother. 2021; 143:112226. [PubMed: 34649352]

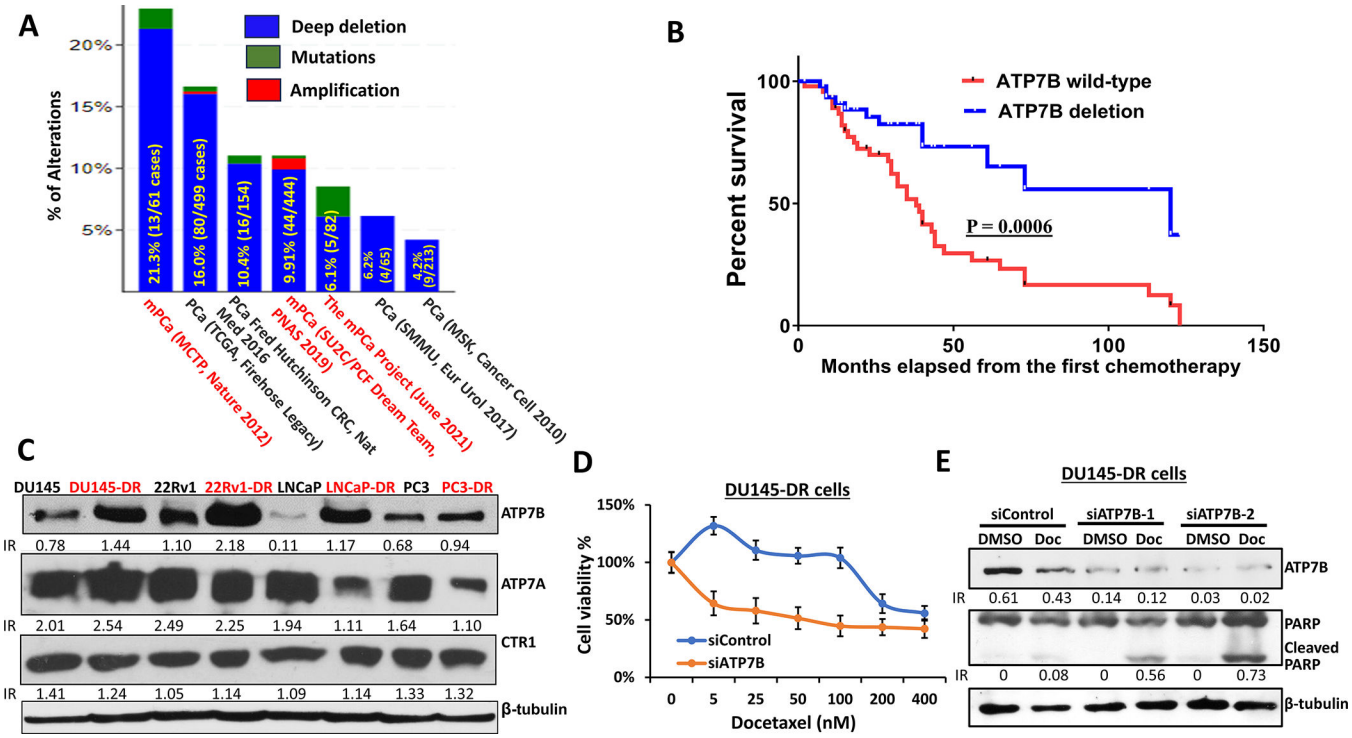

Figure 1.

ATP7B alterations are associated with responses to chemotherapies in PCa patients and with acquired resistance to docetaxel in mPCa cell lines. **A)** Genetic alterations of ATP7B in mPCa and primary PCa specimens from cBioportal databases. **B)** Survival curves of mPCa patients with ATP7B deletion (n=13) or wild type (n=47) after their first chemotherapy. **C)** Western blotting analysis of CTR1, ATP7A, and ATP7B protein expression in docetaxel-resistant vs. parental mPCa cell lines. IR: intensity ratio after adjustment with loading controls. **D & E)** Knock-down of ATP7B expression by siRNAs sensitizes docetaxel-resistant DU145-DR cells to the growth inhibitory effects of docetaxel and the apoptotic effect of docetaxel (1 μM) as indicated by increased PARP cleavage, respectively.

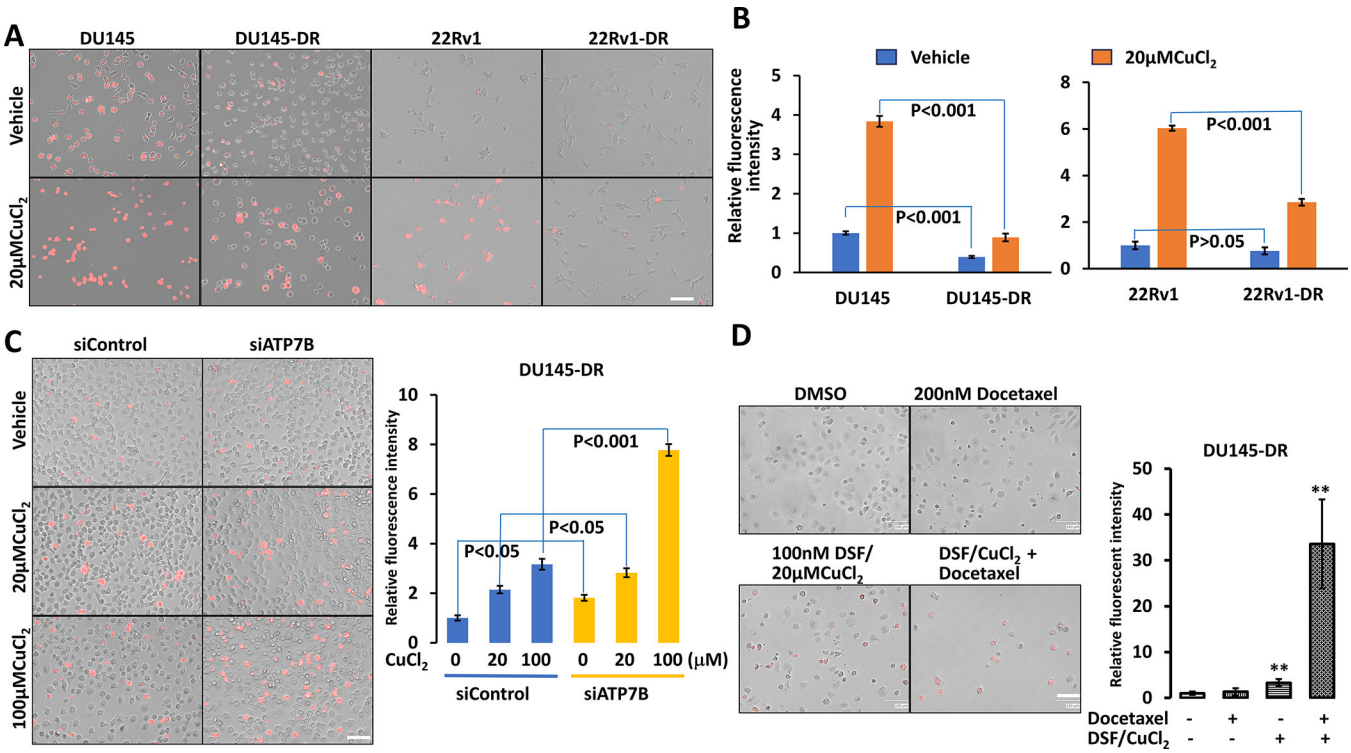

Figure 2.

The uptake of copper is associated with docetaxel responses and ATP7B expression. **A)** Red fluorescence represents cellular copper detected by the CF-4 probe. **B)** Quantitative data of fluorescence intensity are presented by bar figures relative to copper levels in their parental control cell lines and mean ± standard deviations (SDs). Copper levels in parental and DR cells were detected by specific copper probe CF4. **C)** Knock-down of ATP7B expression by siRNAs in docetaxel-resistant DU145 (DU145-DR) cells increases the uptake of cellular copper. **D)** DSF/copper and its combination with docetaxel significantly enhances the uptake of cellular copper in DU145-DR cells. Scale bars in Figures A, C, & D are 100μm.

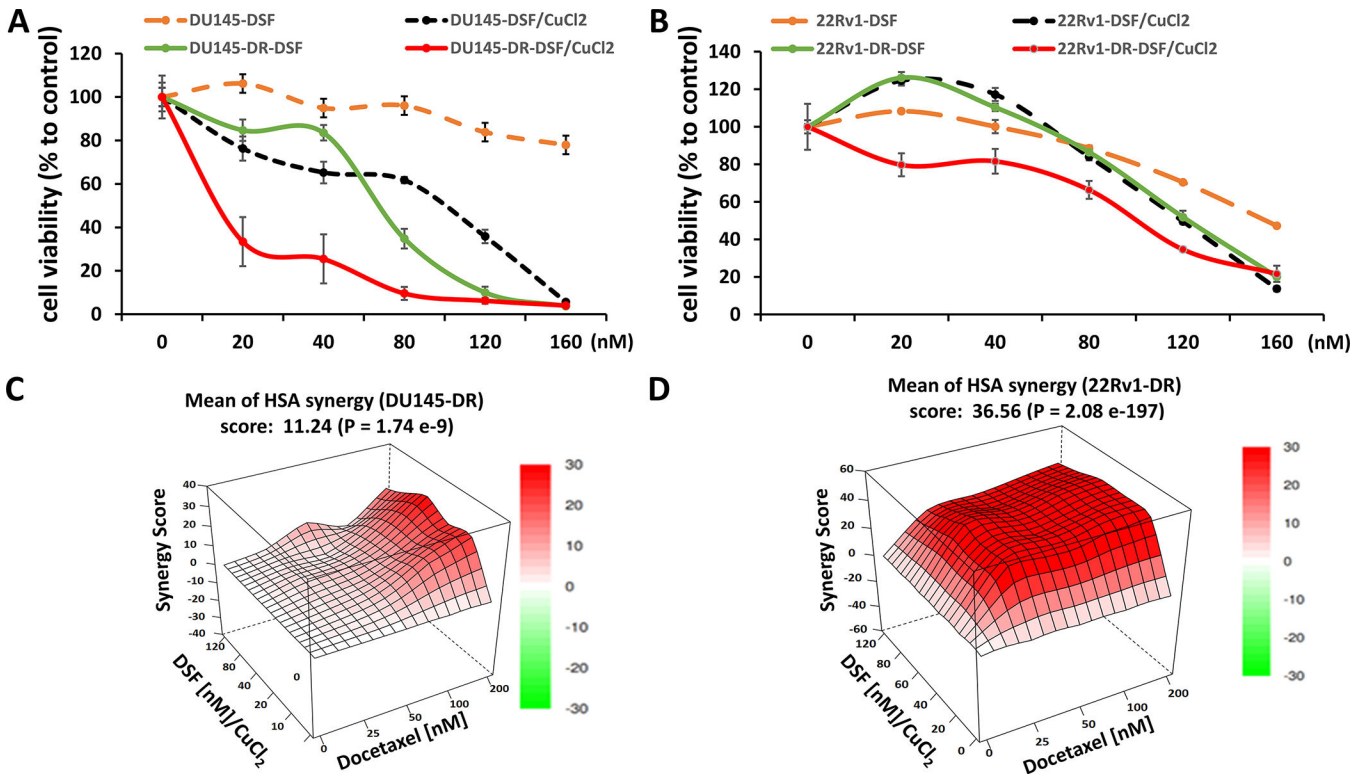

Figure 3.

The effects of DSF, DSF/copper, and the combination of DSF/copper and docetaxel on the growth of 22Rv1-DR and DU145-DR and their parental cell lines. **A & B)** DU145, 22Rv1, DU145-DR, and 22Rv1-DR cells were treated with vehicle control (DMSO), different concentrations of DSF and DSF/$CuCl_2$ as indicated. After 72 h of treatments, cell viability was measured by an MTT assay. **C & D)** The combined effect of DSF/$CuCl_2$ and docetaxel at indicated concentrations on the viability of DU145-DR and 22Rv1-DR cells. The means of HSA synergy scores are shown to be more than 10, indicating synergistic effects. $CuCl_2$ was added at a concentration of 20μM in all the experiments.

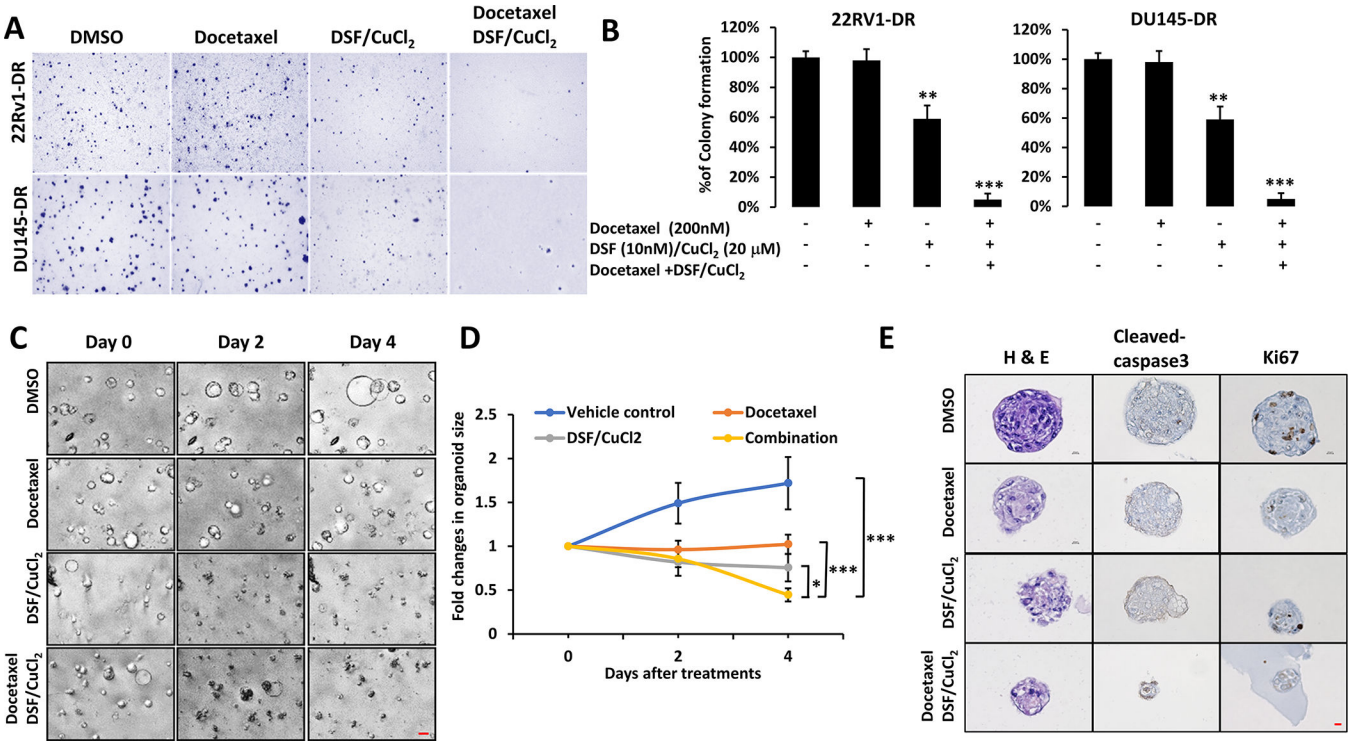

Figure 4.

The effects of DSF, DSF/copper, and the combination of DSF/copper and docetaxel on the growth of 3 dimensional (3D) cultures of docetaxel-resistant cell lines and PCa PDOs. **A & B**) Soft agar colony formation assay with indicted treatments of 22Rv1-DR and DU145-DR cells was performed using 6-well plates and the numbers of colonies were counted at an optimum time of 4 to 6 weeks post-cell seeding. Photos are a qualitative analysis of colony formation. The data are presented by bar figures and mean ± standard deviations (SDs) of four independent wells. **, P<0.01 and ***, P<0.001. **C**) PCa PDOs were treated with 100 nM docetaxel, 500 nM DSF/20μM $CuCl_2$, and the combination of both at indicated times. Photos of PDOs were taken under Keyence BZX710 microscope with a scale bar of 50μm. **D)** Fold changes of PDO sizes relative to those at day 0 were measured and calculated at different time point. Each point represents the mean ± standard deviations (SDs). **E)** H & E and IHC staining of formalin-fixed and histone-embedded PDOs with anti-Ki67 and cleaved Caspase-3 antibodies after the indicated treatments for 4 days were shown with a scale bar of 10μm.

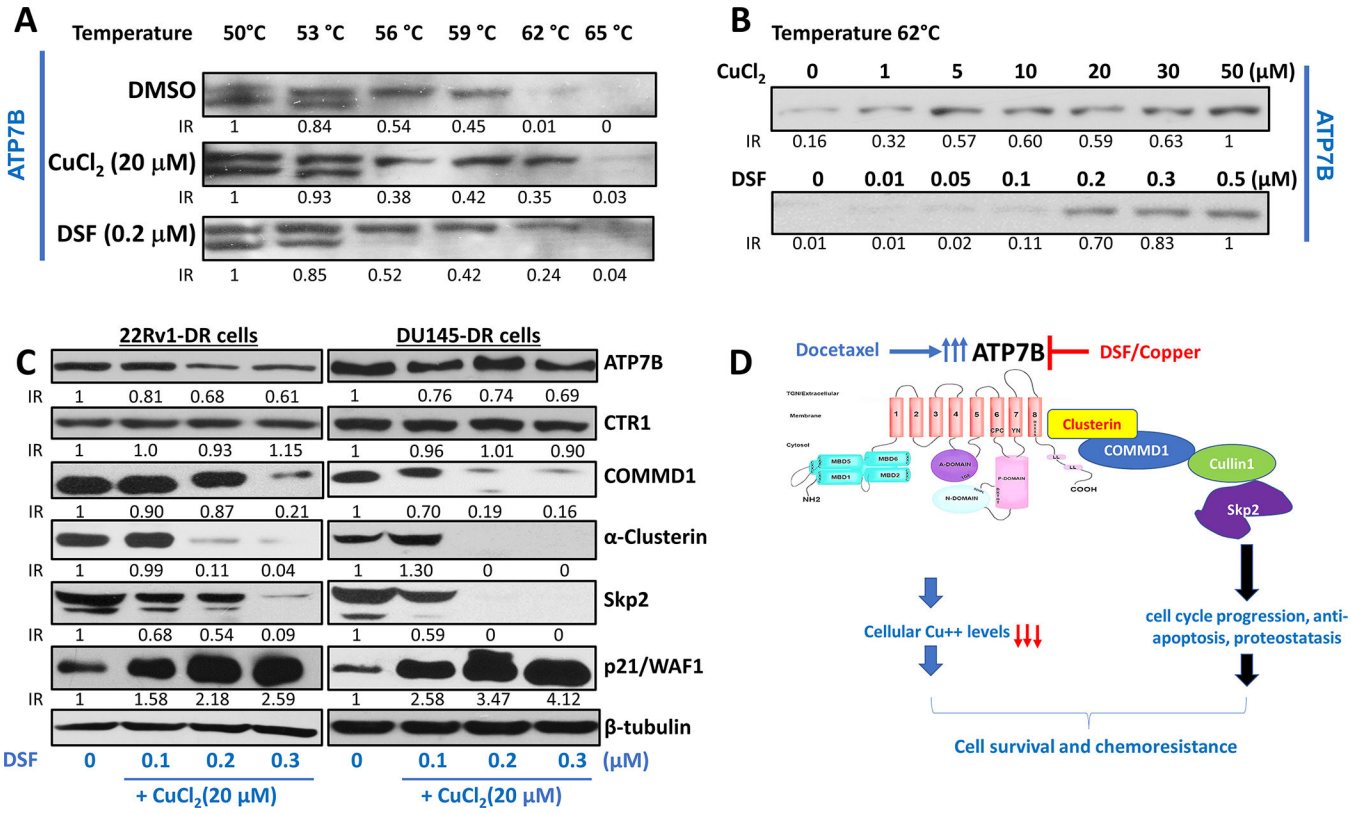

Figure 5.

DSF or copper interacts with ATP7B leading to disruption of its non-canonical down-stream events. **A)** Cellular thermal shift assay was performed using DU145-DR cells treated with 200 nM DSF, 20 μM $CuCl_2$, or DMSO under a range of temperatures from 50 °C to 65 °C. IR: intensity ratio after adjustment with loading controls. **B)** Cellular isothermal dose response was examined on DU145-DR cells at 62 °C and treated with DSF/$CuCl_2$ at indicated concentrations. **C)** Western blotting analysis of non-canonical downstream events of ATP7B in both DU145-DR and 22Rv1-DR cells with indicated treatments for 8 hours. **D)** The proposed and simplified downstream events of ATP7B that were influenced by docetaxel and DSF/$CuCl_2$ treatments.

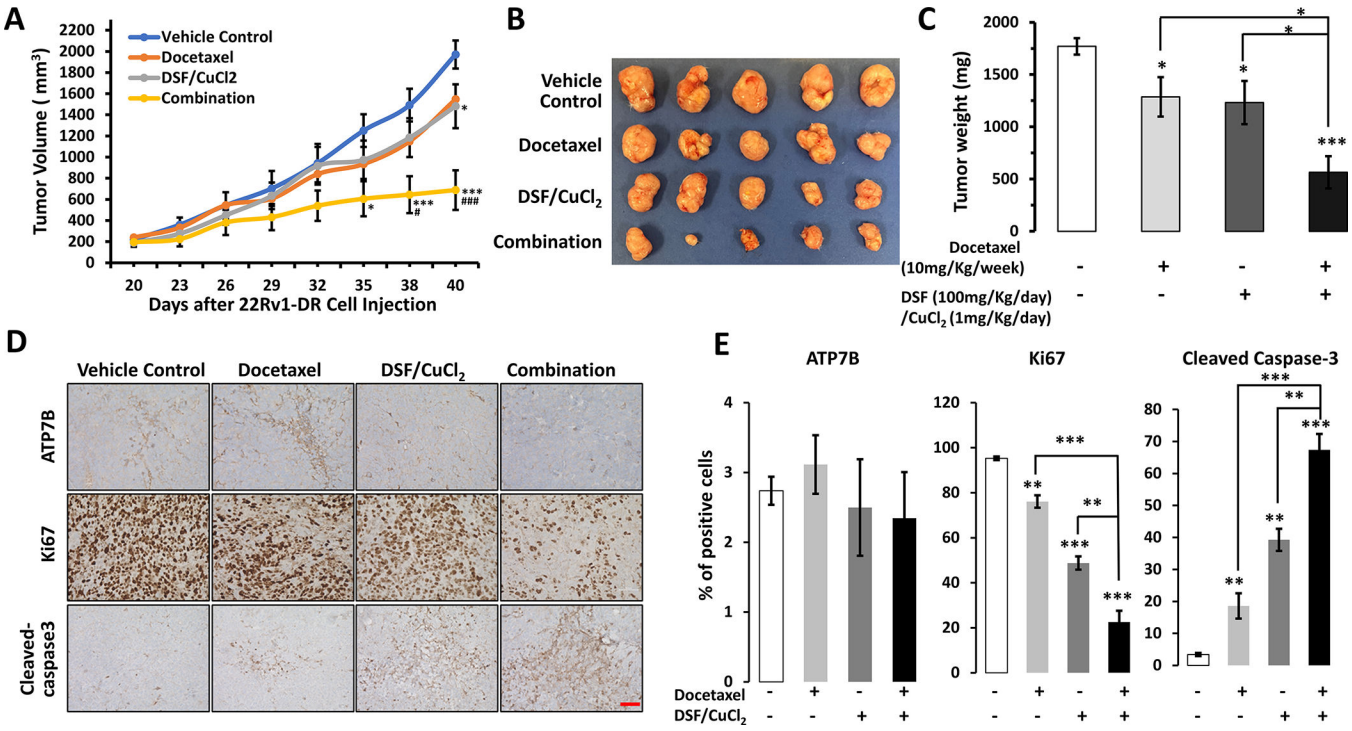

Figure 6.

DSF/copper significantly re-sensitizes the anti-tumor effects of docetaxel in 22Rv1-DR xenograft tumors. Tumor-bearing mice were randomly divided into treatment and control groups with similar tumor sizes in each group. Tumor volumes and weight were recorded and presented as mean ± SD. The tumor volumes were analyzed by two-way ANOVA (**A**) and Photos of excised wet tumors were shown in (**B**). *, $P<0.05$; ***, $P<0.001$; docetaxel, $DSF/CuCl_2$ or the combination versus vehicle control; #, $P<0.05$; ###, P<0.001; combination versus docetaxel or DSF/Cu++. Tumor weights were evaluated by the Student's t-test (**C**). *, $P<0.05$; ***, $P<0.001$. (**D & E**) $DSF/CuCl_2$ and docetaxel plus $DSF/CuCl_2$ demonstrated anti-proliferative effects as indicated by reduced Ki67 staining and apoptotic effects by increased cleaved caspase-3 staining There are no statistical significances among different treatment groups in terms of average staining intensities of ATP7B. Scale bars are 50μm.